

Vibration of Symmetrically Laminated Rectangular Plates Considering Deformation and Rotatory Inertia

J. A. Bowlus*

Air Force Wright Aeronautical Laboratories, Wright-Patterson Air Force Base, Ohio

A. N. Palazotto†

Air Force Institute of Technology, Wright-Patterson Air Force Base, Ohio
and

J. M. Whitney‡

Air Force Wright Aeronautical Laboratories, Wright-Patterson Air Force Base, Ohio

An analytical study was conducted using the Galerkin technique to determine the natural frequencies and mode shapes for symmetrically laminated rectangular plates, considering the effects of shear deformation and rotatory inertia. Two different graphite-epoxy symmetric plates were used in the analysis and three different boundary conditions for each plate, simply supported, clamped, and two opposite sides clamped/two opposite sides simply supported, were considered. Convergence characteristics, comparison to classical results, and the effects of length to thickness ratios were investigated. The finding indicated that as the length to thickness ratios were reduced (a/h , $b/h < 30$ for the first mode), shear deformation effects significantly lowered the natural frequencies. Analysis also showed that rotatory inertia effects were very small. Convergence characteristics for all three boundary conditions were very good, and excellent agreement with the classical solutions was achieved.

Introduction

IN recent years, interest in the use and application of composite materials has greatly increased. This is due in part to their high strength to weight ratios and the fact that they can be tailored for specific applications. Because of their unique properties, they have opened up numerous fields of research and analysis.

Past developments have shown that the dynamic response of composite plates departs more from classical thin plate theory than that of isotropic plates. It has been found that vibration analysis based on this theory yields frequencies that are too high. Therefore, to gain better agreement with reality, the theories used in analyzing the response of composite plates need to include the effects of shear deformation and rotatory inertia.

A number of theories including shear deformation and rotatory inertia have been proposed to date. Mindlin¹ introduced a two-dimensional theory of flexural motion for isotropic elastic plates. Yang et al.² extended Mindlin's plate theory to laminates consisting of an arbitrary number of bonded anisotropic layers (commonly referred to as the YNS theory). They considered the frequency equations for the propagation of harmonic waves in a two-layer, infinite, isotropic plate. Whitney and Pagano³ applied the YNS theory to laminated plates consisting of an arbitrary number of bonded anisotropic layers, each having one plane of symmetry parallel to the central plane of the plate. Using this theory, they presented a closed-form solution for the free vibrations of antisymmetric angle-ply plate strips. Following Whitney and Pagano, Bert and Chen⁴ presented a closed-form solution for the free vibration of simply supported rectangular plates of antisymmetric angle-ply laminates.

In each of these references, the inclusion of shear deformation and rotatory inertia considering boundary conditions other than simple supports was not carried out. In addition, none of these references considered laminates with non-vanishing bending-twisting shear coupling terms. Recent works by Dym and Shames⁵ and Dawe and Craig^{6,7} have considered the vibration of rectangular plates with non-vanishing bending-twisting shear coupling. However, numerical results for such plates were limited to homogeneous, unidirectional composites with the fibers off-axis, relative to the sides of the plate.

In the present paper, three different boundary conditions are considered in conjunction with the Galerkin method for determining the natural frequencies and mode shapes for symmetrically laminated, rectangular plates, including the effects of transverse shear deformation and rotatory inertia. Bending-twisting shear coupling terms are included in the formulation of the problem. Two different graphite-epoxy symmetric plates with $[0/90]_S$ and $[\pm 45]_S$ orientations were used in the analysis. The three different boundary conditions considered for each plate were: simply supported, clamped, and two opposite sides clamped/two opposite sides simply supported. Convergence characteristics, comparison to classical results, and the effects of length to thickness ratios were investigated.

Modeling

Governing Equations

Figure 1 illustrates the standard x , y , z Cartesian coordinate system used herein. The plate thickness and in-plane dimensions are denoted by h , a , and b , respectively. In addition, the plate is composed of an arbitrary number of layers with arbitrary fiber orientation in each layer. The Mindlin-type laminated plate equations^{2,3} for the bending of symmetric, anisotropic laminates are based on the assumed displacement field:

$$u = z\psi_x(x, y, t) \quad v = z\psi_y(x, y, t) \quad w = w(x, y, t) \quad (1)$$

Received July 7, 1986; revision received Jan. 23, 1987. Copyright © American Institute of Aeronautics and Astronautics, Inc., 1987. All rights reserved.

*Formerly, Graduate Student; presently Engineer.

†Professor, Aeronautics and Astronautics. Associate Fellow AIAA.

‡Research Engineer. Associate Fellow AIAA.

where u , v , and w are the x , y , and z coordinate displacements, respectively, and ψ_x and ψ_y are the rotations of a line perpendicular to the midplane due to bending.

The plate moment, shear force, and displacement relations, taken from Ref. 3, and reduced to a form for symmetric laminates (commas denote partial differentiation) are:

$$\begin{Bmatrix} M_x \\ M_y \\ M_{xy} \end{Bmatrix} = \begin{bmatrix} D_{11} & D_{12} & D_{16} \\ D_{12} & D_{22} & D_{26} \\ D_{16} & D_{26} & D_{66} \end{bmatrix} \begin{Bmatrix} \psi_{x,x} \\ \psi_{y,y} \\ \psi_{x,y} \end{Bmatrix} \quad (2)$$

$$\begin{Bmatrix} Q_y \\ Q_x \end{Bmatrix} = k \begin{bmatrix} A_{44} & 0 \\ 0 & A_{55} \end{bmatrix} \begin{Bmatrix} w_{,y} + \psi_y \\ w_{,x} + \psi_x \end{Bmatrix} \quad (3)$$

where k is the shear correction factor introduced by Mindlin. The moments and shear forces are

$$\begin{aligned} (M_x, M_y, M_{xy}) &= \int_{-h/2}^{h/2} (\sigma_x, \sigma_y, \sigma_{xy}) z dz \\ (Q_x, Q_y) &= \int_{-h/2}^{h/2} (\tau_{xz}, \tau_{yz}) dz \end{aligned} \quad (4)$$

and the extensional stiffnesses A_{ij} and the bending stiffnesses D_{ij} are

$$\begin{aligned} A_{ij} &= \int_{-h/2}^{h/2} C_{ij} dz \quad (i, j = 4, 5) \\ D_{ij} &= \int_{-h/2}^{h/2} Q_{ij} dz \quad (i, j = 1, 2, 6) \end{aligned} \quad (5)$$

where C_{ij} are the anisotropic stiffnesses associated with interlaminar shear and Q_{ij} the anisotropic reduced stiffnesses for plane stress.

The governing equations of motion for a plate may be derived by formulating the Lagrangian function (in terms of plate variables) for the plate and applying Hamilton's principle to that Lagrangian. This approach will also yield the required boundary conditions. Reference 8 formulates the Lagrangian for an isotropic plate including the effects of transverse shear and rotatory inertia (modeled using the Mindlin plate theory). Following the derivation from that text and denoting partial derivative with respect to the space variables by a comma and with respect to time by a dot, we have, after applying Hamilton's principle and Green's theorem, the following:

$$\begin{aligned} &\int_{t_1}^{t_2} \int_D [(-I\ddot{\psi}_x + M_{x,x} + M_{xy,y} - Q_x)\delta\psi_x + (-I\ddot{\psi}_y + M_{y,y} \\ &+ M_{xy,x} - Q_y)\delta\psi_y + (-p\ddot{w} + Q_{x,x} + Q_{y,y} + q)\delta w] dA dt \\ &+ \int_{t_1}^{t_2} \int_{\Gamma} [(M_{xy}\delta\psi_x dx - M_x\delta\psi_x dy) + (M_y\delta\psi_y dx \\ &- M_{xy}\delta\psi_y dy) + (Q_y\delta w dx - Q_x\delta w dy)] dt = 0 \end{aligned} \quad (6)$$

where the double integral over the domain represents the equations of motion for the plate and the line integral around the contour represents the required boundary conditions. Also,

$$p = \int_{-h/2}^{h/2} \rho dz \quad I = \int_{-h/2}^{h/2} \rho z^2 dz \quad (7)$$

where ρ is the ply density per unit volume.

To determine the equation of motion for the plate at any time t , we take the double integral expression over the domain and note that the variation cannot be zero over this region. Therefore, the coefficients for each variation coordinate must be equal to zero. Thus, we have

$$\begin{aligned} M_{x,x} + M_{xy,y} - Q_x &= I\ddot{\psi}_x \\ M_{xy,x} + M_{y,y} - Q_y &= I\ddot{\psi}_y \\ Q_{x,x} + Q_{y,y} + q &= \rho\ddot{w} \end{aligned} \quad (8)$$

If we assume the time dependence to be harmonic, then we can separate out the time variable in Eq. (8) and have

$$M_{x,x} + M_{xy,y} - Q_x + \omega^2 I\psi_x = 0 \quad (9)$$

$$M_{xy,x} + M_{y,y} - Q_y + \omega^2 I\psi_y = 0 \quad (10)$$

$$Q_{x,x} + Q_{y,y} + N_x w_{,xx} + 2N_{xy} w_{,xy} + N_y w_{,yy} + \rho\omega^2 w = 0 \quad (11)$$

where ω is the frequency of vibration and $q = N_x w_{,xx} + 2N_{xy} w_{,xy} + N_y w_{,yy}$. This will allow the use of our equations to solve the linear bifurcation problem. We will retain this expression throughout the development but will not consider it when solving the vibration problem. Thus, Eqs. (9–11) are the plate equations of motion.

Before proceeding further, we must determine the appropriate boundary conditions for the system of equations that are sufficient to assure a unique solution. These can be determined from the line integral expression in Eq. (6). The boundary conditions associated with Eq. (9) are represented by $\delta\psi_x$ and its coefficient. Thus we have

$$\int_{\Gamma} (-M_x dy + M_{xy} dx) \delta\psi_x = 0 \quad (12)$$

Similarly, the associated boundary conditions for Eqs. (10) and (11) are, respectively,

$$\int_{\Gamma} (M_y dx - M_{xy} dy) \delta\psi_y = 0 \quad (13)$$

$$\int_{\Gamma} (-Q_x dy + Q_y dx) \delta w = 0 \quad (14)$$

We now have the equations of motion and the required boundary conditions and can proceed with finding a solution for this system.

Galerkin Technique

The Galerkin technique¹¹ will be used to obtain an approximate solution to the set of partial differential equations that describe the motion of the plate. The approach will be to formulate the Galerkin equations, make appropriate substitutions, and then normalize the equations.

In the Galerkin method, we seek a solution to the governing equations in the variational form of Eq. (6). Solutions are assumed to be of the form

$$\begin{aligned} \psi_x &= \sum_{m=1}^M \sum_{n=1}^N A_{mn} \bar{\psi}_{xmn}(xy) \\ \psi_y &= \sum_{m=1}^M \sum_{n=1}^N B_{mn} \bar{\psi}_{ymn}(x,y) \\ w &= \sum_{m=1}^M \sum_{n=1}^N C_{mn} W_{mn}(x,y) \end{aligned} \quad (15)$$

where A_{mn} , B_{mn} , and C_{mn} are undetermined coefficients and the functions ψ_{xmn} , $\bar{\psi}_{ymn}$, and W_{mn} must satisfy the geometric boundary conditions. Taking the first variation with respect to the undetermined coefficients, we obtain the results

$$\begin{aligned}\delta\psi_x &= \sum_{m=1}^M \sum_{n=1}^N \bar{\psi}_{xmn} \delta A_{mn} \\ \delta\psi_y &= \sum_{m=1}^M \sum_{n=1}^N \bar{\psi}_{ymn} \delta B_{mn} \\ \delta w &= \sum_{m=1}^M \sum_{n=1}^N W_{mn} \delta C_{mn}\end{aligned}\quad (16)$$

Substituting Eq. (16) into Eq. (6), collecting terms, and setting the coefficients of δA_{mn} , δB_{mn} , and δC_{mn} equal to zero, we obtain the following set of homogeneous algebraic equations:

$$\begin{aligned}\int_0^b \int_0^a (M_{x,x} + M_{xy,y} - Q_x + \omega^2 I \psi_x) \bar{\psi}_{xpq} dx dy \\ + \int_0^b [M_x(0,y) \bar{\psi}_{xpq}(0,y) - M_x(a,y) \bar{\psi}_{xpq}(a,y)] dy \\ + \int_0^a [M_{xy}(x,0) \bar{\psi}_{xpq}(x,0) - M_{xy}(x,b) \bar{\psi}_{xpq}(x,b)] dx = 0\end{aligned}\quad (17)$$

$$\begin{aligned}\int_0^b \int_0^a (M_{xy,x} + M_{y,y} - Q_y + \omega^2 I \psi_y) \bar{\psi}_{ypq} dx dy \\ + \int_0^b [M_{xy}(0,y) \bar{\psi}_{ypq}(0,y) - M_{xy}(a,y) \bar{\psi}_{ypq}(a,y)] dy \\ + \int_0^a [M_y(x,0) \bar{\psi}_{ypq}(x,0) - M_y(x,b) \bar{\psi}_{ypq}(x,b)] dx = 0\end{aligned}\quad (18)$$

$$\begin{aligned}\int_0^b \int_0^a (Q_{x,x} + Q_{y,y} + N_x w_{,xx} + 2N_{xy} w_{,xy} \\ + N_y w_{,yy} + \rho \omega^2 w) W_{pq} dx dy + \int_0^b [Q_x(0,y) W_{mn}(0,y) \\ - Q_x(a,y) W_{pq}(a,y)] dy + \int_0^a [Q_y(x,0) W_{pq}(x,0) \\ - Q_y(x,b) W_{pq}(x,b)] dx = 0\end{aligned}\quad (19)$$

where $p = 1, 2, \dots, M$ and $q = 1, 2, \dots, M$.

Now substituting the displacement variables in place of the moments and shear forces [from Eqs. (2) and (3)] into Eqs.

Table 1 Stiffness elements for plate 1

Graphite-epoxy [0/90] _S	
Element	Nondimensional value
a_{44}	0.3857174
a_{45}	0
a_{55}	0.385714
d_{11}	1.11083
d_{12}	0.0251509
d_{16}	0
d_{22}	0.23055
d_{26}	0
d_{66}	0.0357143

(17), (18), and (19), we have

$$\begin{aligned}\int_0^a \int_0^b [D_{11} \psi_{x,xx} + 2D_{16} \psi_{x,xy} + D_{66} \psi_{x,yy} + D_{16} \psi_{y,xx} \\ + (D_{12} + D_{66}) \psi_{y,xy} + D_{26} \psi_{y,yy} - kA_{55} \psi_x - kA_{55} w_{,x} + I\omega^2 \psi_x] \\ \times \bar{\psi}_{xpq} dx dy + \int_0^b \{ [D_{11} \psi_{x,x}(0,y) + D_{12} \psi_{y,y}(0,y) \\ + D_{16} (\psi_{x,y}(0,y) + \psi_{y,x}(0,y))] \bar{\psi}_{xpq}(0,y) - [D_{11} \psi_{x,x}(a,y) \\ + D_{12} \psi_{y,y}(a,y) + D_{16} (\psi_{x,y}(a,y) + \psi_{y,x}(a,y))] \bar{\psi}_{xmn}(a,y) \} dy \\ + \int_0^a \{ [D_{16} \psi_{x,x}(x,0) + D_{26} \psi_{y,y}(x,0) + D_{66} (\psi_{x,y}(x,0) \\ + \psi_{y,x}(x,0))] \bar{\psi}_{xpq}(x,0) - [D_{16} \psi_{x,x}(x,b) + D_{26} \psi_{y,y}(x,b) \\ + D_{66} (\psi_{x,y}(x,b) + \psi_{y,x}(x,b))] \bar{\psi}_{xpq}(x,b) \} dx = 0\end{aligned}\quad (20)$$

$$\begin{aligned}\int_0^a \int_0^b [D_{16} \psi_{x,xx} + (D_{12} + D_{66}) \psi_{x,xy} + D_{26} \psi_{x,yy} + D_{66} \psi_{y,xx} \\ + 2D_{26} \psi_{y,xy} + D_{22} \psi_{y,yy} - kA_{44} \psi_y - kA_{44} w_{,y} \\ + I\omega^2 \psi_y] \bar{\psi}_{ypq} dx dy + \int_0^b \{ [D_{16} \psi_{x,x}(0,y) + D_{26} \psi_{y,y}(0,y) \\ + D_{66} (\psi_{x,y}(0,y) + \psi_{y,x}(0,y))] \bar{\psi}_{ypq}(0,y) - [D_{16} \psi_{x,x}(a,y) \\ + D_{26} \psi_{y,y}(a,y) + D_{66} (\psi_{x,y}(a,y) + \psi_{y,x}(a,y))] \bar{\psi}_{ypq}(a,y) \} dy \\ + \int_0^a \{ [D_{12} \psi_{x,x}(x,0) + D_{22} \psi_{y,y}(x,0) + D_{26} (\psi_{x,y}(x,0) \\ + \psi_{y,x}(x,0))] \bar{\psi}_{ypq}(x,0) - [D_{12} \psi_{x,x}(x,b) + D_{22} \psi_{y,y}(x,b) \\ + D_{26} (\psi_{x,y}(x,b) + \psi_{y,x}(x,b))] \bar{\psi}_{ypq}(x,b) \} dx = 0\end{aligned}\quad (21)$$

$$\begin{aligned}\int_0^a \int_0^b (kA_{55} \psi_{x,x} + kA_{55} w_{,xx} + kA_{44} \psi_{y,y} + kA_{44} w_{,yy} \\ - k_2 N_0 w_{,xx} + 2k_3 N_0 w_{,xy} - k_1 N_0 w_{,yy} + \rho \omega^2 w) W_{pq} dx dy \\ + \int_0^b \{ [kA_{55} \psi_x(0,y) + kA_{55} w_{,x}(0,y)] W_{pq}(0,y) \\ - [kA_{55} \psi_x(a,y) + kA_{55} w_{,x}(a,y)] W_{pq}(a,y) \} dy \\ + \int_0^a \{ [kA_{44} \psi_y(x,0) + kA_{44} w_{,y}(x,0)] W_{pq}(x,0) \\ - [kA_{44} \psi_y(x,b) + kA_{44} w_{,y}(x,b)] W_{pq}(x,b) \} dx = 0\end{aligned}\quad (22)$$

where $N_y = -k_1 N_0$, $N_x = -k_2 N_0$, and $N_{xy} = k_3 N_0$. We choose to normalize Eqs. (20–22) by the following scheme:

$$\begin{aligned} d_{ij} &= D_{ij}/E_2 h^3, & a_{ij} &= A_{ij}/E_2 h, & R &= a/b \\ s &= a/h, & \bar{w} &= w/h, & \xi &= x/a, & \eta &= y/b \\ \lambda_1 &= N_0 b^2/E_2 h^3, & \lambda_2 &= \bar{\omega}^2 = \rho a^4 \omega^2/E_2 h^3 \end{aligned}$$

where d_{ij} and a_{ij} are normalized bending and extensional stiffnesses, respectively, E_2 is Young's modulus in the direction normal to the lamina fibers, R the plate aspect ratio, s the length to thickness ratio, ω the normalized frequency, ξ the normalized x coordinate, η the normalized y coordinate, and h the plate thickness. We will also make the substitution

$$\bar{I} = \frac{12}{h^2 p} \int_{-h/2}^{h/2} \rho z^2 dz \quad (23)$$

The reason for this substitution is that it will allow us to construct a laminate of different materials. Thus we can use our homogeneous theory to handle hybrid composite plates. Note that if each ply has the same density ρ , then $\bar{I} = 1$.

After these substitutions and subsequent simplifications, Eqs. (20), (21), and (22) become, respectively,

$$\begin{aligned} & \int_0^1 \int_0^1 [d_{11} \psi_{\xi, \xi \xi} + 2Rd_{16} \psi_{\xi, \xi \eta} + R^2 d_{66} \psi_{\xi, \eta \eta} + d_{16} \psi_{\eta, \xi \xi} \\ & + R(d_{12} + d_{66}) \psi_{\eta, \xi \eta} + R^2 d_{26} \psi_{\eta, \eta \eta} - ks^2 a_{55} \psi_{\xi} - ksa_{55} w_{, \xi} \\ & + (\lambda_2 \bar{I}/12S^2) \psi_{\xi}] \bar{\psi}_{\xi pq} d\xi d\eta + \int_0^1 \{ [d_{11} \psi_{\xi, \xi} (0, \eta) \\ & + Rd_{12} \psi_{\eta, \eta} (0, \eta) + d_{16} (R\psi_{\xi, \eta} (0, \eta) + \psi_{\eta, \xi} (0, \eta))] \bar{\psi}_{\xi pq} (0, \eta) \\ & - [d_{11} \psi_{\xi, \xi} (1, \eta) + Rd_{12} \psi_{\eta, \eta} (1, \eta) + d_{16} (R\psi_{\xi, \eta} (1, \eta) \\ & + \psi_{\eta, \xi} (1, \eta))] \bar{\psi}_{\xi pq} (1, \eta) \} d\eta + \int_0^1 \{ [d_{16} \psi_{\xi, \xi} (\xi, 0) \\ & + Rd_{26} \psi_{\eta, \eta} (\xi, 0) + d_{66} (R\psi_{\xi, \eta} (\xi, 0) + \psi_{\eta, \xi} (\xi, 0))] \bar{\psi}_{\xi pq} (\xi, 0) \\ & - [d_{16} \psi_{\xi, \xi} (\xi, 1) + Rd_{26} \psi_{\eta, \eta} (\xi, 1) + d_{66} (R\psi_{\xi, \eta} (\xi, 1) \\ & + \psi_{\eta, \xi} (\xi, 1))] \bar{\psi}_{\xi pq} (\xi, 1) \} d\xi = 0 \end{aligned} \quad (24)$$

$$\begin{aligned} & \int_0^1 \int_0^1 [d_{16} \psi_{\xi, \xi \xi} + (d_{12} + d_{66}) \psi_{\xi, \xi \eta} + R^2 d_{26} \psi_{\xi, \eta \eta} + d_{66} \psi_{\eta, \xi \xi} \\ & + 2Rd_{26} \psi_{\eta, \xi \eta} + R^2 d_{22} \psi_{\eta, \eta \eta} - ks^2 a_{44} \psi_{\eta} - ksa_{44} w_{, \eta} \\ & + (\lambda_2 \bar{I}/12S^2) \psi_{\eta}] \psi'_{\eta pq} d\xi d\eta + \int_0^1 \{ [d_{16} \psi_{\xi, \xi} (0, \eta) \\ & + Rd_{26} \psi_{\eta, \eta} (0, \eta) + d_{66} (R\psi_{\xi, \eta} (0, \eta) + \psi_{\eta, \xi} (0, \eta))] \bar{\psi}_{\eta pq} (0, \eta) \\ & - [d_{16} \psi_{\xi, \xi} (1, \eta) + Rd_{26} \psi_{\eta, \eta} (1, \eta) + d_{66} (R\psi_{\xi, \eta} (1, \eta) \\ & + \psi_{\eta, \xi} (1, \eta))] \bar{\psi}_{\eta pq} (1, \eta) \} d\eta + \int_0^1 \{ [d_{12} \psi_{\xi, \xi} (\xi, 0) \\ & + Rd_{22} \psi_{\eta, \eta} (\xi, 0) + d_{26} (R\psi_{\xi, \eta} (\xi, 0) + \psi_{\eta, \xi} (\xi, 0))] \bar{\psi}_{\eta pq} (\xi, 0) \\ & - [d_{12} \psi_{\xi, \xi} (\xi, 1) + Rd_{22} \psi_{\eta, \eta} (\xi, 1) + d_{26} (R\psi_{\xi, \eta} (\xi, 1) \\ & + \psi_{\eta, \xi} (\xi, 1))] \bar{\psi}_{\eta pq} (\xi, 1) \} d\xi = 0 \end{aligned} \quad (25)$$

$$\begin{aligned} & \int_0^1 \int_0^1 [ksa_{55} \psi_{\xi, \xi} + ka_{55} w_{, \xi \xi} + kRsa_{44} \psi_{\eta, \eta} + kR^2 a_{44} w_{, \xi \xi} \\ & - k_2 \lambda_1 (R^2/s^2) w_{, \xi \xi} + 2k_3 (R^3/s^2) \lambda_1 w_{, \xi \eta} - k_1 (R^4/s^2) \lambda_1 w_{, \eta \eta} \\ & + (\lambda_2/S^2)] W_{pq} d\xi d\eta + \int_0^1 \{ [ksa_{55} \psi_{\xi} (0, \eta) \\ & + ka_{55} w_{, \xi} (0, \eta)] W_{pq} (0, \eta) - [ksa_{55} \psi_{\xi} (1, \eta) \\ & + ka_{55} w_{, \xi} (1, \eta)] W_{pq} (1, \eta) \} d\eta + \int_0^1 \{ [ksa_{44} \psi_{\eta} (\xi, 0) \\ & + Rka_{44} w_{, \eta} (\xi, 0)] W_{pq} (\xi, 0) - [ksa_{44} \psi_{\eta} (\xi, 1) \\ & + Rka_{44} w_{, \eta} (\xi, 1)] W_{pq} (\xi, 1) \} d\xi = 0 \end{aligned} \quad (26)$$

At this point we are ready to pick a boundary condition, find approximate functions for ψ_x , ψ_y , and w for that condition, and substitute into Eqs (24), (25), and (26). If we could find approximate functions that would satisfy both the geometric and natural boundary conditions, then the boundary integrals in Eqs. (24–26) would vanish. However, finding such functions is extremely difficult, if not impossible. This is particularly true for laminates with nonvanishing shear coupling stiffness A_{45} , D_{16} , and D_{26} . We can find functions that satisfy the geometric boundary conditions. In this case, the boundary integrals in Eqs. (24–26) do not vanish and must be included in the analysis. It should be noted that these boundary integrals also vanish when all of the boundary conditions are geometric in nature, such as in the case of all four clamped boundaries.

Simply Supported Boundary Condition

Since the Galerkin equations have been formulated, it is possible to choose the displacement and rotation functions (w, ψ_x, ψ_y) that satisfy the three equations for each boundary condition being considered. These differential equations can be integrated, resulting in three algebraic equations (for each boundary condition). The eigenvalue problem can be for-

Table 2 Stiffness elements for plate 2

Graphite-epoxy [± 45] _S	
Element	Nondimensional value
a_{44}	0.385714
a_{45}	0
a_{55}	0.385714
d_{11}	0.383635
d_{12}	0.312207
d_{16}	0.22007
d_{22}	0.383635
d_{26}	0.22007
d_{66}	0.32277

mulated and from that the natural frequencies and mode shapes can be obtained.

For a plate simply supported on all sides, we know from plate theory that at

$$x=0, a$$

$$w=\psi_y=0$$

$$M_x = D_{11}\psi_{x,x} + D_{12}\psi_{y,y} + D_{16}(\psi_{y,x} + \psi_{x,y}) = 0 \quad (27)$$

and at

$$y=0, b$$

$$w=\psi_x=0$$

$$M_y = D_{12}\psi_{x,x} + D_{22}\psi_{y,y} + D_{26}(\psi_{y,x} + \psi_{x,y}) = 0 \quad (28)$$

Therefore, we shall choose for our admissible functions (functions that satisfy the geometric boundary conditions and are continuously differentiable one time) in terms of normalized coordinates

$$\begin{aligned} \psi_\xi &= \sum_{m=1}^M \sum_{n=1}^N A_{mn} \cos(m\pi\xi) \sin(n\pi\eta) \\ \psi_\eta &= \sum_{m=1}^M \sum_{n=1}^N B_{mn} \sin(m\pi\xi) \cos(n\pi\eta) \\ w &= \sum_{m=1}^M \sum_{n=1}^N C_{mn} \sin(m\pi\xi) \sin(n\pi\eta) \end{aligned} \quad (29)$$

We now substitute these functions and their appropriate derivatives into Eqs. (24–26). Some discussion is required here to understand the equations resulting from this substitution, integration, and simplification. When substituting for ψ_ξ , ψ_η , and w , the dummy variables m and n represent integer values identifying the different terms in the infinite series. When substituting for $\psi_{\xi pq}$, $\psi_{\eta pq}$, and \bar{W}_{pq} , the dummy variables p and q will be used instead of m and n . This will insure that we will not lose any terms when performing the required multiplications and integration in Eqs. (24–26). Because our assumed functions are made up of sine and cosine functions, and because the argument of each of these consists of an integer multiple of π , we can easily integrate and evaluate these expressions. However, the value of these integrals will depend on the value of m , n , p , and q , whether $m=n$ (or $p=q$), and whether the sum of the integer dummy variables $m+p$ (or $n+q$) is even or odd. Thus, to represent the entire set of Galerkin equations as three equations, the following notation is used. For expressions of the form $(\frac{1}{2}$ or 0) the value on the left side of the “or” results when $m=p$ (or $n=p$) and the value on the right side results when $m \neq p$ (or $n \neq q$). Sometimes the right side of the expression

has the added dependence on whether the sum of $m+p$ (or $n+q$) is even or odd. This will be expressed as (0 or 0 even, $2m$ odd). If the sum is even, then the value marked even results from the integration. Likewise, if the sum is odd, then the value marked odd results. Thus, when we substitute our assumed functions [Eqs. (29)], into Eqs. (24), (25), and (26) and integrate and simplify, we have, from Eq. (24),

$$\begin{aligned} &\sum_{m=1}^M \sum_{n=1}^N \{ \pi^2 (\frac{1}{2} \text{ or } 0) (\frac{1}{2} \text{ or } 0) (-m^2 d_{11} - n^2 R^2 d_{66} \\ &- k s^2 a_{55} / \pi^2 + \lambda_2 \bar{I} / 12 S^2 \pi^2) - (0 \text{ or even, } 2m \text{ odd}) \\ &\times (0 \text{ or } 0 \text{ even, } 2q \text{ odd}) (2Rmnd_{16}) / ((m^2 - p^2)(q^2 - n^2)) \\ &+ (0 \text{ or } 0 \text{ even, } 2q \text{ odd}) [nRd_{16}(1 - \cos(m\pi) \cos(p\pi))] \\ &\div (q^2 - n^2) \} A_{mn} + \{ \pi^2 (\frac{1}{2} \text{ or } 0) (\frac{1}{2} \text{ or } 0) \\ &\times (-mnR(d_{12} + d_{66})) - (0 \text{ or } 0 \text{ even, } 2m \text{ odd}) \\ &\times (0 \text{ or } 0 \text{ even, } 2q \text{ odd}) (m^2 d_{16} + n^2 R^2 d_{26}) \\ &\div ((m^2 - p^2)(q^2 - n^2)) + (0 \text{ or } 0 \text{ even, } 2q \text{ odd}) \\ &\times [md_{16}(1 - \cos(m\pi) \cos(p\pi))] / (q^2 - n^2) \} B_{mn} \\ &- [\pi (\frac{1}{2} \text{ or } 0) (\frac{1}{2} \text{ or } 0) (mksa_{55})] C_{mn} = 0 \end{aligned} \quad (30)$$

from Eq. (25)

$$\begin{aligned} &\sum_{m=1}^M \sum_{n=1}^N \{ \pi^2 (\frac{1}{2} \text{ or } 0) (\frac{1}{2} \text{ or } 0) (-mnR(d_{12} + d_{66})) \\ &- (0 \text{ or } 0 \text{ even, } 2p \text{ odd}) (0 \text{ or } 0 \text{ even, } 2n \text{ odd}) \\ &\times (m^2 d_{16} + n^2 R^2 d_{66}) / ((p^2 - m^2)(n^2 - q^2)) \\ &+ (0 \text{ or } 0 \text{ even, } 2p \text{ odd}) [nRd_{26}(1 - \cos(n\pi))] \\ &\div (p^2 - m^2) \} A_{mn} + \{ \pi^2 (\frac{1}{2} \text{ or } 0) (\frac{1}{2} \text{ or } 0) \\ &\times (-m^2 d_{66} - n^2 R^2 d_{22} - (ks^2 a_{44}) / \pi^2 + \lambda_2 \bar{I} / 12 S^2 \pi^2) \\ &- (0 \text{ or } 0 \text{ even, } 2p \text{ odd}) (0 \text{ or } 0 \text{ even, } 2n \text{ odd}) \\ &\times (2Rmnd_{26}) / ((p^2 - m^2)(n^2 - q^2)) + (0 \text{ or } 0 \text{ even, } 2p \text{ odd}) \\ &\times [md_{26}(1 - \cos(n\pi) \cos(q\pi))] / (p^2 - m^2) \} B_{mn} \\ &- [\pi (\frac{1}{2} \text{ or } 0) (\frac{1}{2} \text{ or } 0) (nRksa_{44})] C_{mn} = 0 \end{aligned} \quad (31)$$

and from Eq. (26)

$$\begin{aligned} &\sum_{m=1}^M \sum_{n=1}^N -\pi (\frac{1}{2} \text{ or } 0) (\frac{1}{2} \text{ or } 0) (mksa_{55}) A_{mn} \\ &- \pi (\frac{1}{2} \text{ or } 0) (\frac{1}{2} \text{ or } 0) (nRksa_{44}) B_{mn} \\ &+ [\pi^2 (\frac{1}{2} \text{ or } 0) (\frac{1}{2} \text{ or } 0) (-m^2 ka_{55} - n^2 Rka_{44} \\ &+ k_2 \lambda_1 m^2 (R^2 / s^2) + k_1 \lambda_1 n^2 (R^4 / s^2 + \lambda_2 / S^2 \pi^2)) \\ &+ (0 \text{ or } 0 \text{ even, } 2p \text{ odd}) (0 \text{ or } 0 \text{ even, } 2q \text{ odd}) \\ &\times (2k_3 mnR^3 \lambda_1) / (s^2 (p^2 - m^2)(q^2 - n^2))] C_{mn} = 0 \end{aligned} \quad (32)$$

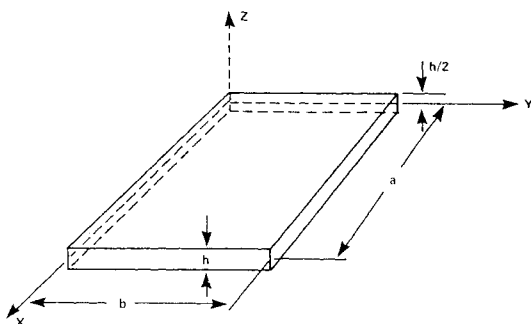


Fig. 1 Plate geometry.

Equations (30–32) represent the entire set of Galerkin equations for the simply supported boundary and are now ready to be programmed. The process to generate the set of Galerkin equations is to pick an M and N (they must be equal) and then create an equation for every combination of p and q .

It should be noted that Eq. (29) is an exact solution for orthotropic plates ($A_{45} = D_{16} = D_{26} = 0$) without inplane shear loading ($k_3 = 0$). For this special case, Eqs. (30–32) can be uncoupled to produce $M \times N$ sets of three equations involving the coefficients A_{mn} , B_{mn} , and C_{mn} . Thus, an independent set is produced for each value of m and n . The same set of equations can be obtained by substituting Eq. (29) into the equations of motion [Eqs. (9–11)]. This is anticipated, as the Galerkin method will produce an exact solution when the assumed displacement functions coincide with the exact solution.

Clamped Boundary Condition

For a plate clamped on all sides, one knows from plate theory that at

$$\begin{aligned} x=0, a \\ w=\psi_x=\psi_y=0 \end{aligned} \quad (33)$$

and at

$$\begin{aligned} y=0, b \\ w=\psi_x=\psi_y=0 \end{aligned} \quad (34)$$

Therefore, we shall choose for our admissible functions in terms of normalized coordinates

$$\begin{aligned} \psi_\xi &= \sum_{m=1}^M \sum_{n=1}^N A_{mn} \sin(m\pi\xi) \sin(n\pi\eta) \\ \psi_\eta &= \sum_{m=1}^M \sum_{n=1}^N B_{mn} \sin(m\pi\xi) \sin(n\pi\eta) \\ W &= \sum_{m=1}^M \sum_{n=1}^N C_{mn} \sin(m\pi\xi) \sin(n\pi\eta) \end{aligned} \quad (35)$$

As before, substituting these functions and their appropriate derivatives into Eqs. (24), (25), and (26), and in-

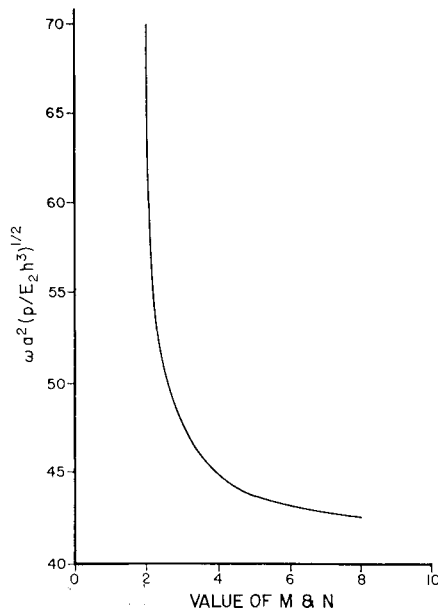


Fig. 2 Normalized frequency vs M and N ; plate 2 (clamped boundary—third mode).

tegrating, simplifying, and taking only a finite number of terms, we have from Eq. (24)

$$\begin{aligned} \sum_{m=1}^M \sum_{n=1}^N [\pi^2(\frac{1}{2} \text{ or } 0)(\frac{1}{2} \text{ or } 0)(-m^2 d_{11} - n^2 R^2 d_{66} \\ - ks^2 a_{55}/\pi^2 + \lambda_2 \bar{I}/12S^2 \pi^2) - (0 \text{ or } 0 \text{ even}, 2p \text{ odd}) \\ \times (0 \text{ or } 0 \text{ even}, 2q \text{ odds})(2Rmnd_{16})/(p^2 - m^2) \\ \times (q^2 - n^2))] A_{mn} + [\pi^2(\frac{1}{2} \text{ or } 0)(\frac{1}{2} \text{ or } 0)(-m^2 d_{16} \\ - n^2 R^2 d_{26}) + (0 \text{ or } 0 \text{ even}, 2p \text{ odd})(0 \text{ or } 0 \text{ even}, 2q \text{ odd}) \\ \times (mnR(d_{12} + d_{66}))/((p^2 - m^2)(q^2 - n^2))] B_{mn} \\ - [\pi(0 \text{ or } 0 \text{ even}, 2p \text{ odd})(\frac{1}{2} \text{ or } 0) \\ \times (mksa_{55})/(p^2 - m^2)] C_{mn} = 0 \end{aligned} \quad (36)$$

from Eq. (25)

$$\begin{aligned} \sum_{m=1}^M \sum_{n=1}^N [\pi^2(\frac{1}{2} \text{ or } 0)(\frac{1}{2} \text{ or } 0)(-m^2 d_{16} - n^2 R^2 d_{26}) \\ - (0 \text{ or } 0 \text{ even}, 2p \text{ odd})(0 \text{ or } 0 \text{ even}, 2q \text{ odd}) \\ \times (mnR(d_{12} + d_{66}))/((p^2 - m^2)(q^2 - n^2))] A_{mn} \\ + [\pi^2(\frac{1}{2} \text{ or } 0)(\frac{1}{2} \text{ or } 0)(-m^2 d_{66} - n^2 R^2 d_{22} \\ - (ks^2 a_{44})/\pi^2 + \lambda_2 \bar{I}/12S^2 \pi^2) \\ + (0 \text{ or } 0 \text{ even}, 2p \text{ odd})(0 \text{ or } 0 \text{ even}, 2q \text{ odd}) \\ \times (2Rmnd_{26})/((p^2 - m^2)(q^2 - n^2))] B_{mn} \\ - [\pi(\frac{1}{2} \text{ or } 0)(0 \text{ or } 0 \text{ even}, 2q \text{ odd}) \\ \times (nRksa_{44})/(q^2 - n^2)] C_{mn} = 0 \end{aligned} \quad (37)$$

and from Eq. (26)

$$\begin{aligned} \sum_{m=1}^M \sum_{n=1}^N -\pi(0 \text{ or } 0 \text{ even}, 2p \text{ odd})(\frac{1}{2} \text{ or } 0) \\ \times (mksa_{55})/(p^2 - m^2) A_{mn} + \pi(\frac{1}{2} \text{ or } 0) \\ \times (0 \text{ or } 0 \text{ even}, 2q \text{ odd})(nRksa_{44})/(q^2 - n^2) B_{mn} \\ + [\pi^2(\frac{1}{2} \text{ or } 0)(\frac{1}{2} \text{ or } 0)(-m^2 ka_{55} - n^2 R^2 ka_{44} \\ + k_2 \lambda_1 m^2 (R^2/s^2) + k_1 \lambda_1 n^2 (R^4/s^2 + \lambda_2/S^2 \pi^2)) \\ + (0 \text{ or } 0 \text{ even}, 2p \text{ odd})(0 \text{ or } 0 \text{ even}, 2q \text{ odd}) \\ \times (2k_3 mnR^3 \lambda_1)/(s^2(p^2 - m^2)(q^2 - n^2))] C_{mn} = 0 \end{aligned} \quad (38)$$

Equations (36–38) are now ready to be programmed to generate the Galerkin equations as before.

Clamped, Simply Supported Boundary Condition

For a plate clamped on two opposite sides and simply supported on two opposite sides, one has the following boundary conditions; at

$$\begin{aligned} x=0, a \\ w=\psi_x=\psi_y=0 \end{aligned} \quad (39)$$

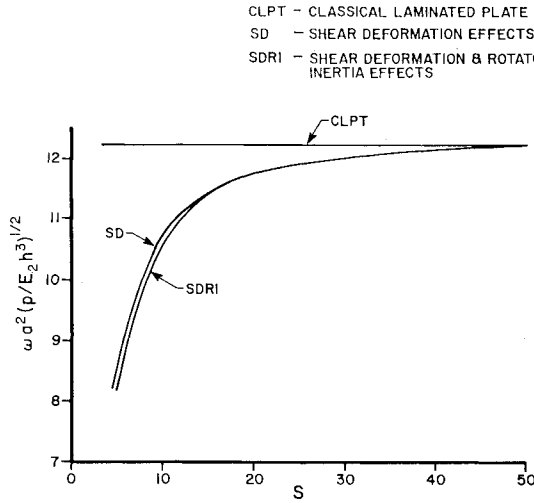


Fig. 3 Normalized frequency vs thickness ratio; plate 1 (simply supported boundary—first mode).

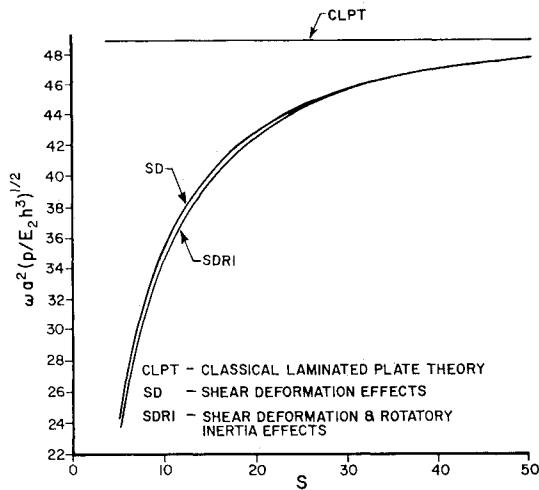


Fig. 4 Normalized frequency vs thickness ratio; plate 1 (simply supported boundary—fifth mode).

and at

$$y=0, b$$

$$w = \psi_{x,x} = 0$$

$$M_y = D_{12} \psi_{x,x} + D_{22} \psi_{y,y} + D_{26} (\psi_{y,x} + \psi_{x,y}) = 0 \quad (40)$$

Therefore, we shall choose for our admissible functions in terms of normalized coordinates

$$\begin{aligned} \psi_\xi &= \sum_{m=1}^M \sum_{n=1}^N A_{mn} \sin(m\pi\xi) \sin(n\pi\eta) \\ \psi_\eta &= \sum_{m=1}^M \sum_{n=1}^N B_{mn} \sin(m\pi\xi) \cos(n\pi\eta) \\ W &= \sum_{m=1}^M \sum_{n=1}^N C_{mn} \sin(m\pi\xi) \sin(n\pi\eta) \end{aligned} \quad (41)$$

As before, substituting these functions and their appropriate derivatives into Eqs. (24), (25), and (26), and integrating, simplifying, and taking only a finite number of

terms, we have the following equations:

From Eq. (24)

$$\begin{aligned} \sum_{m=1}^M \sum_{n=1}^N [& \pi^2 (\frac{1}{2} \text{ or } 0) (\frac{1}{2} \text{ or } 0) (-m^2 d - n^2 R^2 d \\ & - ks^2 a / \pi^2 + \lambda_2 \bar{I} / 12 S^2 \pi^2) + (0 \text{ or } 0 \text{ even}, 2p \text{ odd}) \\ & \times (0 \text{ or } 0 \text{ even}, 2q \text{ odd}) (2Rmnd_{16}) / ((p^2 - m^2) \\ & \times (q^2 - n^2))] A_{mn} - [\pi (0 \text{ or } 0 \text{ even}, 2p \text{ odd}) \\ & \times (\frac{1}{2} \text{ or } 0) (mnR(d_{12} + d_{66})) / (p^2 - m^2) \\ & - \pi (\frac{1}{2} \text{ or } 0) (0 \text{ or even}, 2q \text{ odd}) (m^2 d_{16} \\ & + n^2 R^2 d_{26}) / (q^2 - n^2)] B_{mn} - [(0 \text{ or } 0 \text{ even}, 2p \text{ odd}) \\ & \times (\frac{1}{2} \text{ or } 0) (mksa_{55}) / (p^2 - m^2)] C_{mn} = 0 \end{aligned} \quad (42)$$

from Eq. (25)

$$\begin{aligned} \sum_{m=1}^M \sum_{n=1}^N \{ & \pi (0 \text{ or } 0 \text{ even}, 2p \text{ odd}) (\frac{1}{2} \text{ or } 0) (mnR(d_{12} \\ & + d_{66})) / (p^2 - m^2) - \pi (\frac{1}{2} \text{ or } 0) (0 \text{ or } 0 \text{ even}, 2n \text{ odd}) \\ & \times (m^2 d_{16} + n^2 R^2 d_{26}) / (n^2 - q^2) + \pi (\frac{1}{2} \text{ or } 0) \\ & \times [nRd_{26}(1 - \cos(n\pi) \cos(q\pi))] \} A_{mn} + [\pi^2 (\frac{1}{2} \text{ or } 0) \\ & \times (\frac{1}{2} \text{ or } 0) (-m^2 d_{66} - n^2 R^2 d_{22} - (ks^2 a_{44}) / \pi^2 \\ & + \lambda_2 \bar{I} / 12 S^2 \pi^2) - (0 \text{ or } 0 \text{ even}, 2p \text{ odd}) \\ & \times (0 \text{ or } 0 \text{ even}, 2n \text{ odd}) (2Rmnd_{26}) / ((p^2 - m^2) \\ & \times (n^2 - q^2)) + (0 \text{ or } 0 \text{ even}, 2p \text{ odd}) \\ & \times [md_{26}(1 - \cos(n\pi) \cos(q\pi))] / (p^2 - m^2)] B_{mn} \\ & - [\pi (\frac{1}{2} \text{ or } 0) (\frac{1}{2} \text{ or } 0) (nRksa_{44})] C_{mn} = 0 \end{aligned} \quad (43)$$

and from Eq. (26)

$$\begin{aligned} \sum_{m=1}^M \sum_{n=1}^N (& 0 \text{ or } 0 \text{ even}, 2p \text{ odd}) (\frac{1}{2} \text{ or } 0) (mksa_{55}) \\ & \div (p^2 - m^2) A_{mn} - \pi (\frac{1}{2} \text{ or } 0) (\frac{1}{2} \text{ or } 0) (nRksa_{44}) B_{mn} \\ & + [\pi^2 (\frac{1}{2} \text{ or } 0) (\frac{1}{2} \text{ or } 0) (-m^2 ka_{55} - n^2 R^2 ka_{44} \\ & + k_2 \lambda_1 m^2 (R^2 / s^2) + k_1 \lambda_1 n^2 (R^4 / s^2 + \lambda_2 / S^2 \pi^2)) \\ & + (0 \text{ or } 0 \text{ even}, 2p \text{ odd}) (0 \text{ or } 0 \text{ even}, 2p \text{ odd}) \\ & \times (2k_3 mnR^3 \lambda_1) / (s^2 (p^2 - m^2) (q^2 - n^2))] C_{mn} = 0 \end{aligned} \quad (44)$$

Equations (42-44) are now ready to be programmed to generate the Galerkin equations as before. The eigenvalue $[A]\bar{x} = \lambda[B]\bar{x}$, where $[A]$ is the stiffness matrix and $[B]$ the combined mass and inertia matrix, can now be easily formulated with the three Galerkin equations and solved to determine the frequencies and mode shape.

Discussion and Results

Several different characteristics of both the Galerkin technique and shear deformation and rotatory inertia effects

were investigated. To explore the Galerkin technique, convergence characteristics and a comparison to closed-form solutions were researched. To study the effects of shear deformation and rotatory inertia, several cases varying in length to thickness ratio were investigated. We will begin our discussion by describing the type of plates used in the subsequent analysis.

Laminated Plate Properties

Two different types of laminated plates were used in this paper. Both consisted of a graphite-epoxy material (AS/3501) with the following properties:

$$\begin{aligned} E_1/E_2 &= 15, & G_{12}/E_2 &= G_{13}/E_2 = 0.4286 \\ G_{23}/E_2 &= 0.3429, & \nu_{12} &= 0.4 \end{aligned} \tag{45}$$

One plate had a ply layup of $[0/90]_S$ and the second had a layup of $[\pm 45]_S$. Tables 1 and 2 contain the stiffness elements.

The shear correction factor is chosen as the classical value $k=5/6$. For the $[0/90]_S$ laminate, some improved accuracy may be obtained by using two shear correction factors, one associated with A_{55} and another associated with A_{44} . A procedure for determining these shear correction factors for orthotropic laminates has been previously outlined.^{9,10} The improved accuracy by utilizing two shear correction factors is likely to be marginal, except for very thick plates ($a/h, b/h \leq 5$). Thus, the classical values are utilized in conjunction with all numerical results presented in this paper.

Galerkin Technique Characteristics

In using the Galerkin technique for solving the set of three coupled partial differential equations, we have to ask two questions: 1) Does the technique converge to a solution? 2) How does the solution compare with accepted theory? We will now examine these two questions.

A discussion of the proof of convergence for the Galerkin technique may be found in Ref. 11. A criterion based on the method for convergence is whether the assumed functions form a complete set of functions. No attempt to prove convergence will be presented for the work completed herein. However, we will show the necessary (but not sufficient) condition that the frequency drops by smaller and smaller amounts as the values of M and N are increased. Tables 3 and 4 show the values of the normalized frequency

$[\omega a^2(p/E_2 h^3)]$ for the three boundary conditions considered for the two plates with increasing values of M and N . The tables are based on a length to thickness ratio of 20. Boundary condition 1 is the simply supported case; boundary condition 2 is the clamped case; and boundary condition 3 is the clamped (two opposite sides) simply supported (two opposite sides) case.

As can be seen in Table 3, the simply supported case for the $[0/90]_S$ layup is an exact solution. This is to be expected as this laminate is orthotropic. All of the other cases have not converged but display characteristics that make one believe they will converge as M and N get larger. That is, for every increase in M and N , the normalized frequency drops by a smaller and smaller amount.

These tables are by no means offered as proof of convergence, but they do display good convergence characteristics. They also point out a drawback with the Galerkin method. As M and N increase, the computer memory space required to generate the mass and stiffness matrices and to solve the eigenvalue problem becomes quite large. Thus, if one wants a very accurate answer, particularly for a higher mode, one will need the appropriate computer resources.

A plot of the normalized frequency vs M and N for boundary condition 2 for the $[\pm 45]_S$ plate (third mode) is presented in Fig. 2. This condition tends to have one of the worst convergence tendencies of the group. However, even

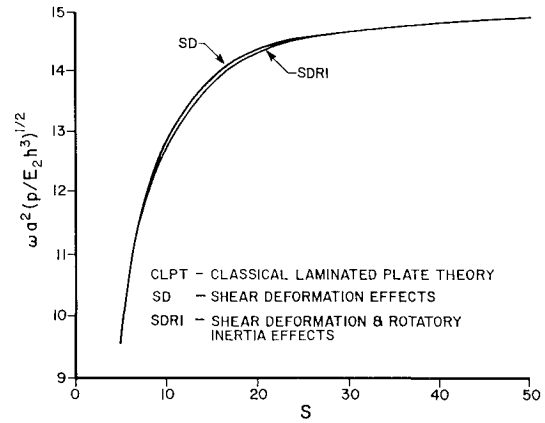


Fig. 5 Normalized frequency vs thickness ratio; plate 2 (simply supported boundary—first mode).

Table 3 Normalized frequencies for plate 1

Nondimensional natural frequencies $[0/90]_S$ graphite-epoxy, $a/b = 1$, $s = 20$				
M	N	First mode	Third mode	Fifth mode
Boundary condition 1 (exact solution)				
2	2	11.758	36.866	—
4	4	11.758	36.866	42.573
6	6	11.758	36.866	42.573
8	8	11.758	36.866	42.573
Boundary condition 2				
2	2	31.751	69.038	—
4	4	23.7341	49.403	67.560
6	6	22.992	48.569	57.062
8	8	22.776	48.328	55.665
Boundary condition 3				
2	2	24.870	65.306	—
4	4	21.235	45.463	52.438
6	6	20.814	45.256	51.832
8	8	20.697	45.225	51.664

Table 4 Normalized frequencies for plate 2

Nondimensional natural frequencies $[\pm 45]_S$ graphite-epoxy, $a/b = 1$, $s = 20$				
M	N	First mode	Third mode	Fifth mode
Boundary condition 1				
2	2	14.699	36.164	—
4	4	14.418	35.444	57.883
6	6	14.283	34.734	55.082
8	8	14.205	34.613	54.856
Boundary condition 2				
2	2	31.091	69.925	—
4	4	22.363	44.553	72.156
6	6	21.412	42.964	64.264
8	8	21.110	42.449	63.095
Boundary condition 3				
2	2	24.300	66.437	—
4	4	18.956	41.549	59.675
6	6	18.337	40.438	58.116
8	8	18.126	40.061	57.673

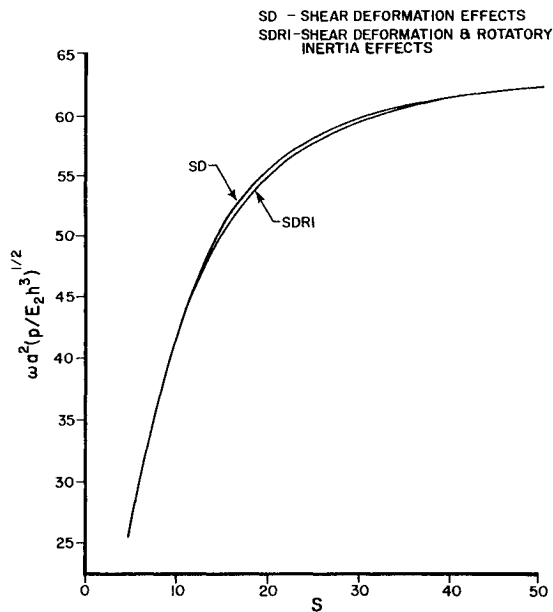


Fig. 6 Normalized frequency vs thickness ratio; plate 2 (simply supported boundary—fifth mode).

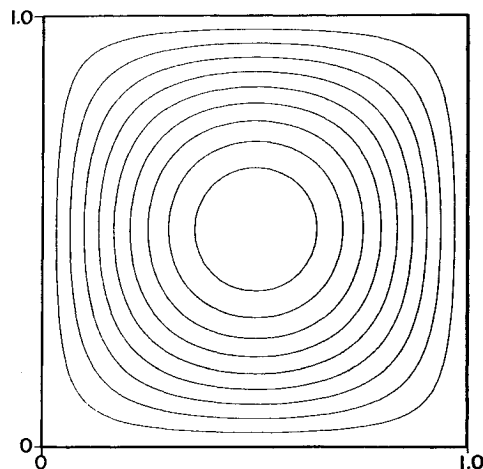


Fig. 7 Mode shape simply supported boundary; plate 1 (first mode).

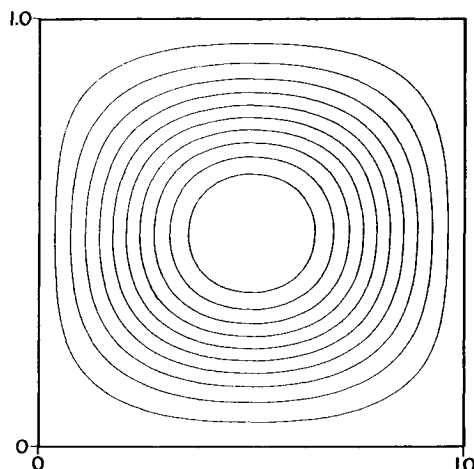


Fig. 8 Mode shape clamped boundary; plate 1 (first mode).

this condition shows good convergence behavior. In this regard, the choice of functions to represent boundary conditions must be considered. For such boundary conditions in conjunction with classical laminated plate theory, the mode shapes associated with the free vibration of beams have been found to be quite satisfactory.¹² For the present case, however, the beam functions would be those associated with the Timoshenko beam theory, which includes rotatory inertia and transverse shear deformation. Such functions are not very convenient to use. For example, these beam modes are a function of the material properties and the span-to-depth ratio of the beam. Each time one of these parameters is changed, a new beam mode function must be generated. The current choice of assumed functions is convenient, and the numerical results indicate that they are adequate.

The next question deals with the accuracy of the numerical results generated here. We will address this issue by investigating a very long, narrow plate. There are several reasons for this. First, because of the nature of the system of equations for our plate, we can zero out the rotatory inertia, but we cannot zero out the shear deformation effect. When shear deformation is eliminated, the equations become very ill-conditioned and the eigenvalue problem cannot be solved. Therefore, we must look to commonly accepted theory that includes either shear deformation or shear deformation and rotatory inertia effects. We would also like to find a simply supported case for an orthotropic plate because our Galerkin method represents an exact solution for this case. Reference 3 did contain a closed-form solution for an infinitely long, simply supported, orthotropic plate including shear deformation effects, and this is what the authors used to validate their program.

From Ref. 3, we have

$$\omega_m = \omega'_m (1 - D_{11} m^2 \pi^2) / (D_{11} m^2 \pi^2 + k A_{55} a^2) \quad (46)$$

where

$$\omega'_m = (D_{11} m^4 \pi^4 / \rho a^4)^{1/2} \quad (47)$$

Here ω'_m is the natural frequency calculated from the classical theory based on the Kirchhoff hypothesis. If we use the properties for plate 1 (Table 1) and compute the fundamental frequency in normalized form for an infinitely long plate, we obtain

$$\omega'_m a^2 (\rho / E_2 h^3)^{1/2} = 10.402$$

$$\omega_m a^2 (\rho / E_2 h^3)^{1/2} = 8.983 \quad (48)$$

The authors cannot place an infinitely long plate into their Galerkin algorithm. However, we can use a very long plate such as one with $a/b = 20$. From Ref. 2 we can compute the natural frequency without shear deformation and rotatory effects from

$$\omega^2 \rho = D_{11} (\alpha_1^4 / a^4) + 2(D_{12} + 2D_{66}) / (\alpha_2 / a^2 b^2) + D_{22} (\alpha_3^4 / b^4) \quad (49)$$

where

$$\alpha_1 = m\pi \quad \alpha_2 = n\pi \quad \alpha_3 = mn\pi \quad (50)$$

for all m and n (m and n determine the mode).

Again using the properties of Table 1 for our plate with $a/b = 20$, we have

$$\omega_m a^2 (\rho / E_2 h^3)^{1/2} = 10.400 \quad (51)$$

This compares to 10.402 for Whitney's infinitely long plate, so we can conclude that our plate reasonably approximates an infinitely long one and therefore use Eq. (46) to compare

with our Galerkin solution. Table 5 shows the comparison between the closed-form solution and the output from the Galerkin method. As can be seen, excellent agreement was obtained. Table 5 also shows the effect of rotatory inertia for this condition.

It should be noted that the Galerkin method as formulated in the present case from variational principles is equivalent to the Rayleigh-Ritz method.⁹ That is, if our current assumed functions were employed with the Rayleigh-Ritz method, we would arrive at the same set of homogeneous algebraic equations as in the present case with the Galerkin method. Thus, both methods would produce identical numerical results. However, the Galerkin method is more convenient to apply than the Rayleigh-Ritz method.

Shear Deformation and Rotatory Inertia Effects

The second area of investigation was to determine the effect of shear deformation and rotatory inertia for the boundary conditions considered. This was accomplished by varying the length to thickness ratio and comparing those results to classical laminated plate theory. Only square plates were considered.

For the simply supported $[0/90]_S$ plate, the length to thickness ratio was varied from 5 to 50. The results are plotted in Figs. 3 and 4 as the normalized frequency vs the thickness ratio for the first and fifth bending modes. It can

be seen that shear deformation effects can be significant (up to 33% lower for the first mode and 52% lower for the fifth mode for a length to thickness ratio of 5) while rotatory inertia effects account for only 2% lower frequency at the worst point. Notice that as the length to thickness ratio approaches 50, we asymptotically approach the classical laminated solution.

These same trends are seen for the $[\pm 45]_S$ simply supported plate. Figures 5 and 6 plot the normalized frequency vs the length to thickness ratio for the first and fifth modes for this plate. Although the frequencies are slightly higher, the same behavior occurs as before. The shear deformation effect becomes significant for length to thickness ratios of less than 35, and rotatory inertia effects are very small. Table 6 presents this idea. There were no classical solutions available to compare these results but, based on the behavior of the first plate, we could estimate a first-mode normalized frequency of about 15 and fifth-mode normalized frequency of about 63.

Table 5 Galerkin method and closed-form solution

Mode	Comparison of plate 1 Nondimensional frequency $\omega a^2(p/E_2 h^3)^{1/2}$		
	Closed-form solution with SD	Galerkin method with SD no RI	Galerkin method with SD and RI
		$M = N = 5$	
1	8.98	8.98	8.96
2	8.99	8.99	8.97
3	9.00	9.00	8.98
4	9.01	9.01	8.99
5	9.03	9.03	9.01

Note: SD = shear deformation, RI = rotatory inertia.

Table 6 Shear deformation (SD) and rotatory inertia (RI) effects for plate 2^a

<i>s</i>	Nondimensional frequency $\omega a^2(p/E_2 h^3)^{1/2}$			
	First mode		Fifth mode	
	SD no RI	SD and RI	SD no RI	SD and RI
5	9.62	9.57	25.66	25.51
10	12.83	12.77	42.06	41.69
15	13.88	13.84	50.79	50.39
20	14.31	14.28	55.42	55.08
25	14.53	14.51	58.05	57.77
30	14.65	14.63	59.65	59.43
35	14.72	14.71	60.67	60.49
40	14.76	14.75	61.37	61.23
50	14.88	14.87	62.23	62.13

^aClassical laminated plate frequency: none available. Simply supported boundary condition $[\pm 45]_S$, $M = N = 6$.

Table 7 Comparison of shear deformation (SD) and rotatory inertia (RI) effects on classical laminated plate theory^a

<i>s</i>	Nondimensional frequency $\omega a^2(p/E_2 h^3)^{1/2}$			
	First mode		Fifth mode	
	SD no RI	SD and RI	SD no RI	SD and RI
5	10.89	10.85	25.10	24.82
10	17.27	17.21	41.44	41.01
15	20.89	20.84	51.30	50.86
20	23.03	23.00	57.45	57.06
25	24.39	24.36	61.53	61.21
30	25.32	25.30	65.23	65.00
35	26.01	25.99	68.09	67.93

^aClassical laminated plate frequency: first mode: 26.47, fifth mode: 74.25. Clamped boundary condition $[0/90]_S$, $M = N = 6$.

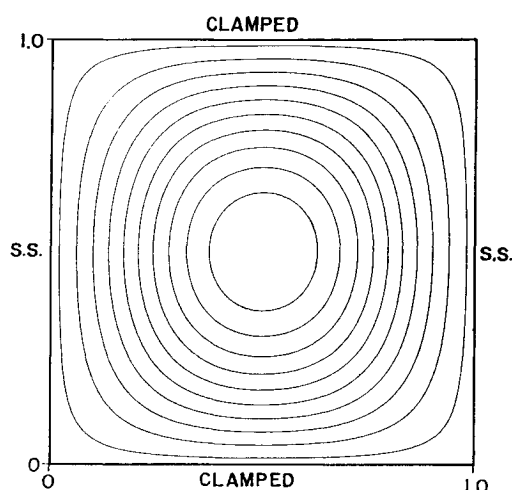


Fig. 9 Mode shape clamped simply supported boundary; plate 1 (first mode).

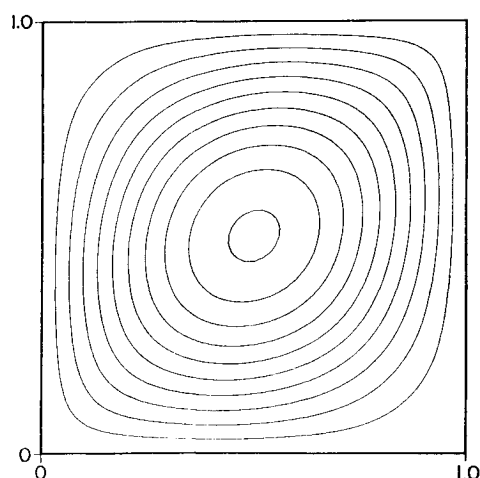


Fig. 10 Mode shape simply supported boundary; plate 2 (first mode).

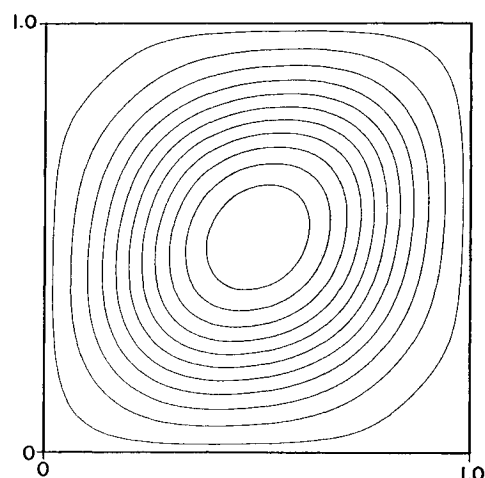


Fig. 11 Mode shape clamped boundary; plate 2 (first mode).

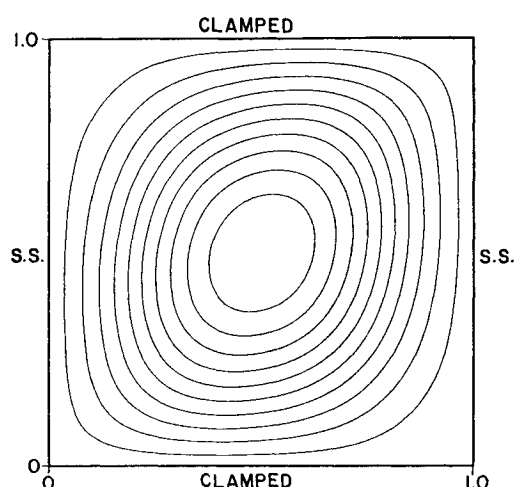


Fig. 12 Mode shape clamped simply supported boundary; plate 2 (first mode).

Table 8 Comparison of shear deformation (SD) and rotatory inertia (RI) effects on classical laminated plate theory^a

s	Nondimensional frequency $\omega a^2(\rho/E_2 h^3)^{1/2}$			
	First mode		Fifth mode	
	SD no RI	SD and RI	SD no RI	SD and RI
5	9.50	9.41	24.26	23.96
10	15.25	15.20	36.80	36.28
15	18.76	18.72	45.12	44.86
20	20.85	20.81	52.09	51.83
25	22.16	22.13	56.97	56.77
30	23.05	23.03	60.48	60.31
35	23.70	23.68	63.08	62.94

^aClassical laminated plate frequency: first mode: 24.53, fifth mode: 70.26. Clamped simply supported boundary condition $[0/90]_S$, $M=N=6$.

Tables 7 and 8 show the comparisons for the second and third boundary conditions for the $[0/90]_S$ plate. They too show the same type of trends as the previous two cases. Shear deformation is a significant effect below length to thickness ratios of 30, and rotatory inertia has little effect on these bending modes.

Mode Shape Determination

When we solved the eigenvalue problem, we also got back the values of the undetermined coefficients used to determine the mode shapes for a particular frequency (this includes the

torsional modes as well). Figures 7-12 are contour plots of the first modes for both plates using all three boundary conditions. A length to thickness ratio of 10 was used in generating these plots.

The verification of these mode shapes, due to the specific material properties, could not be found in the literature. Reference 12 does indicate a similar shape for the totally clamped plate with $[0/90]_S$ and $[\pm 45]_S$ orientations and a E_1/E_2 ratio very close to that used herein. Agreement with this condition appears to be quite good.

Conclusions

Based on the analysis conducted herein, the following conclusions can be made:

1) The Galerkin technique is a valid approach to solving the plate equations of motion for the boundaries considered and is a viable alternative approach to the finite-element method.

2) The natural frequency for a simply supported square orthotropic plate for the first mode is 10% lower than the classical laminated plate theory (CLPT) frequency at a length to thickness ratio (represented by s) of 11 and drops to 33% lower for an s of 5. For the fifth mode, the frequency is 10% lower at an s of 23 and drops to 52% lower for an s of 5.

3) For a cross-ply laminate with the same conditions as in the preceding case, the same type of shear deformation effects were seen. No CLPT solution was found in the current literature; therefore no comparison could be made.

4) The natural frequency for a square orthotropic plate, clamped on all sides, for the first mode, is 10% lower than the CLPT frequency for an s of 21 and drops to 59% lower for an s of 5. For the fifth mode, the frequency is 10% lower at an s of 33 and drops to 66% lower for an s of 5.

5) The natural frequency for a square orthotropic plate, clamped on two opposite sides, simply supported on two opposite sides, for the first mode, is 10% lower than the CLPT frequency for an s of 25 and drops to 61% lower for an s of 5. For the fifth mode, the frequency is 10% lower at an s of 35 and drops to 65% lower for an s of 5.

6) The effects of shear deformation are more significant for the two clamped boundary conditions than for the simply supported boundary.

7) The effects of shear deformation increase with increasing mode for all three boundary conditions.

8) Analysis shows that rotatory inertia has very little effect for all three boundary conditions.

References

- ¹Mindlin, R. D., "Influence of Rotatory Inertia and Shear on Flexural Motions of Isotropic, Elastic, Plates," *Journal of Applied Mechanics*, Vol. 18, March 1951, pp. 31-38.
- ²Yang, P. C., Norris, C. H., and Stavsky, Y., "Elastic Wave Propagation in Heterogeneous Plates," *International Journal of Solids and Structures*, Vol. 2, 1966, pp. 665-684.
- ³Whitney, J. M. and Pagano, N. J., "Shear Deformation in Heterogeneous Anisotropic Plates," *Journal of Applied Mechanics*, Vol. 37, Dec. 1970, pp. 1031-1036.
- ⁴Bert, C. W. and Chen, T. L. C., "Effect of Shear Deformation on Vibration of Antisymmetric Angle-Ply Laminated Rectangular Plates," *International Journal of Solids and Structures*, Vol. 14, 1978, pp. 465-473.
- ⁵Craig, T. J. and Dawe, D. J., "Flexural Vibration of Symmetrically Laminated Composite, Rectangular Plates Including

Transverse Shear Effects," *International Journal of Solids and Structures*, Vol. 22, 1986, pp. 155-169.

⁶Dawe, D. J. and Craig, T. J., "The Influence of Shear Deformation on the Natural Frequencies of Laminated Rectangular Plates," *Composite Structures*, Vol. 3, edited by I. H. Marshall, Elsevier Applied Science Publishers, London, England, 1985, pp. 660-676.

⁷Dawe, D. J. and Craig, T. J., "The Vibration and Stability of Symmetrically-Laminated Composite Rectangular Plates Subjected to In-Plane Stresses," *Composite Structures*, Vol. 5, 1986, pp. 281-307.

⁸Dym, C. L. and Shames, I. H., *Solid Mechanics: A Variational*

Approach, McGraw-Hill, New York, 1973.

⁹Chow, T. S., "On the Propagation of Flexural Waves in an Orthotropic Laminated Plate and Its Response to an Impulsive Load," *Journal of Composite Materials*, Vol. 5, 1971, pp. 306-319.

¹⁰Whitney, J. M., "Shear Correction Factors for Orthotropic Plates Under Static Load," *Journal of Applied Mechanics*, Vol. 40, 1973, pp. 302-304.

¹¹Kantorovich, L. V. and Krylov, V. I., *Approximate Methods of Higher Analysis*, Interscience, New York, 1958.

¹²Whitney, J. M., *Structural Analysis of Laminated Plates*, Technomic Publishing, Lancaster, PA, 1987.

From the AIAA Progress in Astronautics and Aeronautics Series . . .

TRANSONIC AERODYNAMICS—v. 81

Edited by David Nixon, Nielsen Engineering & Research, Inc.

Forty years ago in the early 1940s the advent of high-performance military aircraft that could reach transonic speeds in a dive led to a concentration of research effort, experimental and theoretical, in transonic flow. For a variety of reasons, fundamental progress was slow until the availability of large computers in the late 1960s initiated the present resurgence of interest in the topic. Since that time, prediction methods have developed rapidly and, together with the impetus given by the fuel shortage and the high cost of fuel to the evolution of energy-efficient aircraft, have led to major advances in the understanding of the physical nature of transonic flow. In spite of this growth in knowledge, no book has appeared that treats the advances of the past decade, even in the limited field of steady-state flows. A major feature of the present book is the balance in presentation between theory and numerical analyses on the one hand and the case studies of application to practical aerodynamic design problems in the aviation industry on the other.

Published in 1982, 669 pp., 6×9, illus., \$45.00 Mem., \$75.00 List

TO ORDER WRITE: Publications Dept., AIAA, 370 L'Enfant Promenade S.W., Washington, D.C. 20024-2518